Monthly Notices of the ROYAL ASTRONOMICAL SOCIETY

MNRAS **544,** 975–987 (2025) https://doi.org/10.1093/mnras/staf1685
Advance Access publication 2025 November 6

Strong progenitor age bias in supernova cosmology – II. Alignment with DESI BAO and signs of a non-accelerating universe

Junhyuk Son,★ Young-Wook Lee ,★ Chul Chung ,★ Seunghyun Park and Hyejeon Cho
Department of Astronomy & Center for Galaxy Evolution Research, Yonsei University, Seoul 03722, Korea

Accepted 2025 September 29. Received 2025 September 28; in original form 2025 August 28

ABSTRACT

Supernova (SN) cosmology is based on the key assumption that the luminosity standardization process of Type Ia SNe remains invariant with progenitor age. However, direct and extensive age measurements of SN host galaxies reveal a significant (5.5σ) correlation between standardized SN magnitude and progenitor age, which is expected to introduce a serious systematic bias with redshift in SN cosmology. This systematic bias is largely uncorrected by the commonly used mass-step correction, as progenitor age and host galaxy mass evolve very differently with redshift. After correcting for this age bias as a function of redshift, the SN data set aligns more closely with the w_0w_a cold dark matter (CDM) model recently suggested by the Dark Energy Spectroscopic Instrument (DESI) baryon acoustic oscillations (BAO) project from a combined analysis using only BAO and cosmic microwave background (CMB) data. This result is further supported by an evolution-free test that uses only SNe from young, coeval host galaxies across the full redshift range. When the three cosmological probes (SNe, BAO, and CMB) are combined, we find a significantly stronger ($>9\sigma$) tension with the ΛCDM model than that reported in the DESI papers, suggesting a time-varying dark energy equation of state in a currently non-accelerating universe.

Key words: supernovae: general – galaxies: evolution – cosmological parameters – dark energy – cosmology: observations.

1 INTRODUCTION

Recent baryon acoustic oscillation (BAO) measurements from the Dark Energy Spectroscopic Instrument (DESI) project (A. G. Adame et al. 2025; DESI Collaboration 2025), when combined with cosmic microwave background (CMB) data from the Planck Collaboration V (2020), Planck Collaboration VI (2021), and Atacama Cosmology Telescope (ACT) Data Release 6 (DR6; N. MacCrann et al. 2024; M. S. Madhavacheril et al. 2024; F. J. Qu et al. 2024), exhibit a 3.1σ deviation from the Λ cold dark model (ΛCDM) model. Notably, this result does not support the standard model of dark energy, the cosmological constant, but instead favours a time-varying dark energy equation of state. A significant yet not widely recognized outcome drawn from the DESI BAO analysis is that the cosmological parameters obtained by combining BAO and CMB data alone indicate values ($w_0 = -0.42$, $w_a = -1.75$, $\Omega_{\rm m} = 0.353$; see table 5 of DESI Collaboration 2025) that favour not only a decelerated expansion for the future universe but also suggest a sign of decelerated expansion ($q_0 = 0.092 \pm 0.20$; see Section 5 below) even at the present time, rather than an accelerated expansion. Only when the Type Ia supernova (SN Ia) data set (D. Brout et al. 2022; DES Collaboration 2024; D. Rubin et al. 2025) is added to the BAO and CMB measurements does the present universe remain in a state of accelerated expansion, as is widely recognized (A. G. Riess et al. 1998; S. Perlmutter et al. 1999), even though the future universe will transition to a state of decelerated expansion.

However, this result was obtained without incorporating the supernova (SN) progenitor age-bias effect in the SN data set. In recent years, direct age measurements of SN host galaxies have revealed a significant correlation between the standardized SN magnitude and progenitor age, which is expected to cause a serious systematic bias with redshift in SN cosmology (Y. Kang et al. 2020; Y.-W. Lee et al. 2020, 2022). These results, obtained from host galaxy samples at low redshift ($z < 0.2$), have been repeatedly confirmed by other investigators (K. D. Zhang et al. 2021; J. Wang, Z. Huang & L. Huang 2023). Paper I of this series (C. Chung et al. 2025) further confirms this age bias in the SN distance scale at a 5.5σ level, based on new age measurements for a larger sample of host galaxies across a broader redshift range ($z < 0.45$), illustrating the robustness and universal nature of this systematic bias.

In this paper, in light of the DESI BAO study, we investigate the impact of incorporating the progenitor age-bias effect on SN cosmology when combining the DESI BAO results with the SN data set. We first examine how the redshift-dependent age bias alters the distribution of SN data on the Hubble diagram. Subsequently, within the flat w_0w_aCDM model, we examine the changes that arise after applying the age-bias correction when using the DESI BAO results together with the SN data set. Finally, when all three cosmological probes (SNe, BAO, and CMB) are combined, we present how the cosmological outcomes regarding the accelerated expansion and the cosmological constant would vary depending on whether the age-bias effect is corrected in SN cosmology.

★ E-mail: sonjunhyuk@yonsei.ac.kr (JS); ywlee2@yonsei.ac.kr (YWL); chulchung@yonsei.ac.kr (CC)

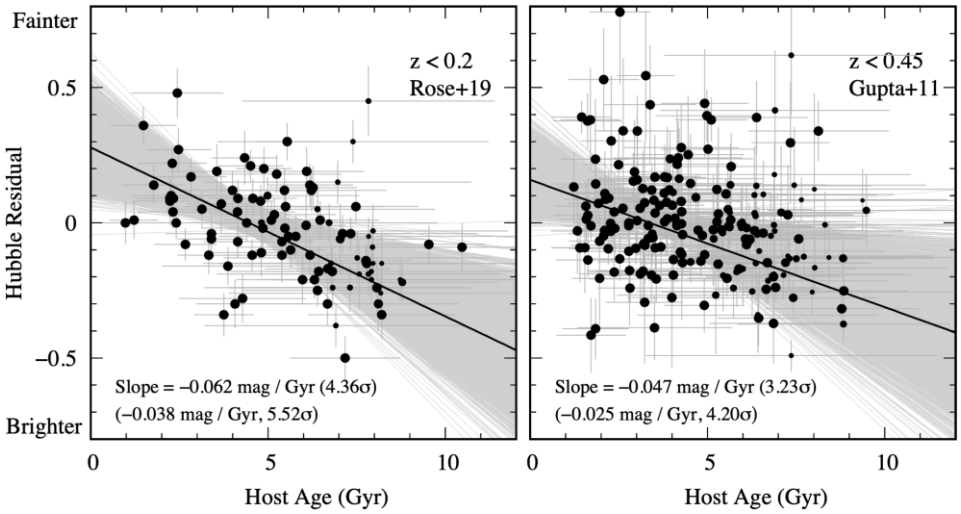

Figure 1. Correlation between population age and HR for SN host galaxies based on our new age measurements reported in Paper I (C. Chung et al. 2025). The HR is a measure of relative luminosity when the SN sample is confined to a narrow redshift range. The left panel shows the R19 sample, for which the strong significance of the correlation was originally reported by Y.-W. Lee et al. (2020) and has been repeatedly confirmed by third parties at the $>5\sigma$ level (K. D. Zhang et al. 2021; J. Wang et al. 2023). The right panel shows a larger sample ($N \sim 200$) of host galaxies (from G11 sample) over a broader redshift range ($z < 0.45$), confirming the universal nature of the age bias. The results shown are based on the LINMIX analysis, while the slopes and significances obtained from the full age posteriors are given in parentheses (see C. Chung et al. 2025).

2 ROBUST EVIDENCE FOR STRONG PROGENITOR AGE BIAS IN THE SUPERNOVA DISTANCE SCALE

Many studies reported in the literature have shown that the standardized magnitude of SN Ia varies with the properties of the host galaxy (P. L. Kelly et al. 2010; M. Sullivan et al. 2010; Y. C. Pan et al. 2014; M. Rigault et al. 2020; D. Brout & D. Scolnic 2021; P. Wiseman et al. 2023, and references therein). However, only a few studies have used directly measured population ages of host galaxies to investigate whether the SN progenitor age is the root cause of this variation. J. S. Gallagher et al. (2008), R. R. Gupta et al. (2011), J. Johansson et al. (2013), and B. M. Rose, P. M. Garnavich & M. A. Berg (2019) explored this issue using low signal-to-noise ratio (S/N) spectra or multiband photometric data for host galaxies, but did not reach a definitive conclusion. The first notable evidence of an age bias in the SN distance scale was presented based on high-precision (S/N = 175) spectroscopic observations of early-type host galaxies (Y. Kang et al. 2020). In this study, three different population synthesis models were applied, each producing consistent results showing that the post-standardization magnitudes of SNe from younger host galaxies are systematically fainter than those from older galaxies. However, due to the limited sample size, restricted to nearby normal early-type host galaxies, the statistical significance of these results was at most around 3σ. Subsequently, Y.-W. Lee et al. (2020) obtained a correlation with much higher statistical significance (4.3σ), based on the B. M. Rose et al. (2019, hearafter R19) sample of host galaxies encompassing all morphological types. This finding was later confirmed by third-party validations from K. D. Zhang et al. (2021) and J. Wang et al. (2023). Recently, in Paper I of this series (C. Chung et al. 2025), we performed new and consistent measurements of population ages for the R19 and R. R. Gupta et al. (2011, hearafter G11) host galaxy samples using the latest version of the population synthesis model from C. Conroy & J. E. Gunn (2010). This analysis further revealed a statistically significant correlation of up to 5.5σ between host age and Hubble residual (HR), underscoring that the age bias is a robust and ubiquitous effect that should be considered a critical systematic bias in SN cosmology (see Fig. 1).

The origin of this correlation between progenitor age and HR has been explained by Y.-W. Lee et al. (2022), who has shown that, unlike the key assumption of SN cosmology (S. W. Jha, K. Maguire & M. Sullivan 2019), the M. M. Phillips (1993) relation (width–luminosity relation, WLR) and the colour–luminosity relation (CLR) in the SN luminosity standardization process do strongly depend on progenitor age at the 4.6σ level. They also found that two subgroups based on other host properties – such as stellar mass, metallicity, and dust content – exhibit only insignificant (0.98σ–1.25σ) offsets in the WLR and CLR, suggesting that progenitor age is most likely the root cause of the reported correlations between host properties and HR. This result is based on the R19 sample at relatively low redshift ($z < 0.20$), but a comparable result is also obtained from the G11 sample at higher redshift ($z < 0.45$), further illustrating the universal nature of this age bias (Park et al., in preparation). C. Chung et al. (2023) also reported that the root cause of the host mass step (P. L. Kelly et al. 2010; M. Sullivan et al. 2010), the property most widely included in SN Ia luminosity standardization, is the stellar population age, based on the empirical galaxy colour–magnitude relation. A more detailed analysis focused on how the linear correlation between progenitor age and HR leads to the mass step and the star formation rate step (M. Rigault et al. 2020) in SN Ia magnitudes will be presented in Paper III of this series (Park et al., in preparation). It is important to note that the luminosity corrections based on the commonly considered host mass step cannot account for the progenitor age-bias effect (see Section 4.3 below). This is because host mass and age evolve very differently with redshift. Within the redshift range most relevant to SN cosmology ($0.0 < z < 1.0$), the evolution of host mass is relatively small (J. B. Bell et al. 2004; C. Conroy, S. Ho & M. White 2007), whereas the evolution of host age is significant – amounting to 5–6 Gyr (M. J. Childress, C. Wolf & H. J. Zahid 2014; Y.-W. Lee et al. 2022). However, the effect of progenitor age bias is still not adequately accounted for in most SN cosmology studies.

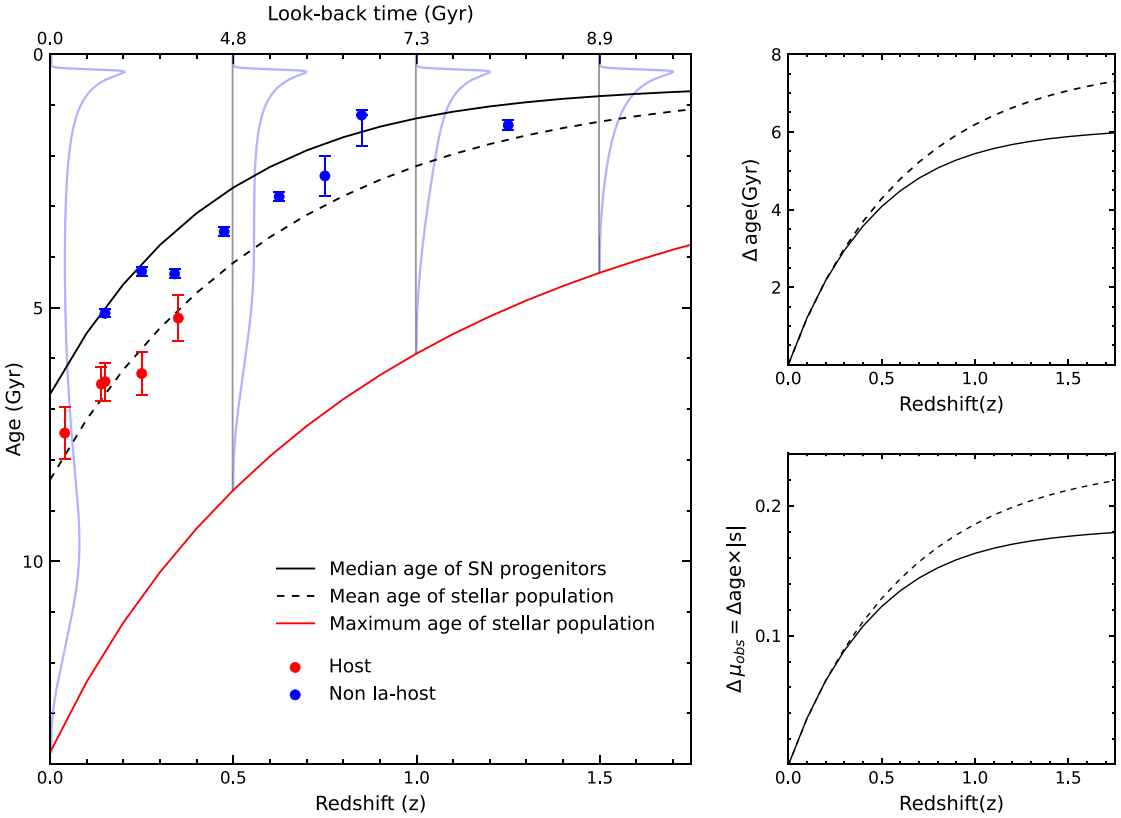

Figure 2. Evolution of stellar population age with redshift. The result is similar to fig. 6 of Y.-W. Lee et al. (2022), but for the w_0w_aCDM model, as suggested by a combined analysis of DESI BAO and CMB (DESI Collaboration 2025). The distribution functions (blue lines) at $z = 0.0$, 0.5, 1.0, and 1.5 represent the SPADs. The black solid line indicates the median age of SN progenitors, while the black dashed line shows the mass-weighted mean age of the stellar population, obtained from the CSFH and compared with the observed data (red and blue circles). In the right panels, the solid and dashed lines show, respectively, the redshift evolution of the median progenitor age and the mean stellar population age, relative to $z = 0$, and the corresponding variations in HR, obtained by multiplying the age difference with the age-bias slope $|s|$.

In the following section, we investigate how and to what extent the progenitor age bias impacts SN cosmology analyses. To do so, we use the average value of the age-bias slopes from previously reported results across three different samples. For the Y. Kang et al. (2020), the weighted mean of the slopes obtained from three population synthesis models is $s = -0.025 \pm 0.006$ mag Gyr^{-1}. For the R19 and G11 samples, the new results obtained by C. Chung et al. (2025) are $s = -0.038 \pm 0.007$ mag Gyr^{-1} and $s = -0.025 \pm 0.006$ mag Gyr^{-1}, respectively (see Fig. 1). We adopt the average value, -0.030 ± 0.004 mag Gyr^{-1}, of these three results from different host galaxy samples at different redshift bins.

3 REDSHIFT EVOLUTION OF PROGENITOR AGE AND ITS COSMOLOGICAL IMPACT

The progenitor age bias in the SN distance scale, as described in the previous section, propagates into a strong redshift-dependent bias in SN magnitudes due to the redshift evolution of progenitor age. This connection was already acknowledged in the original discovery papers (A. G. Riess et al. 1998; B. P. Schmidt et al. 1998; S. Perlmutter et al. 1999). For example, A. G. Riess et al. (1998) stated, 'we can place empirical constraints on the effect that a change in the progenitor age would have on our SN Ia distances by comparing subsamples of low-redshift SNe Ia believed to arise from old and young progenitors'. Therefore, part of the variation in HRs with increasing redshift, as observed in the residual Hubble diagram, results from the redshift evolution of progenitor age.[1] Accordingly, a correction is required to remove this effect in order to isolate the purely cosmological signal. The most direct approach for correcting this effect would be to measure the ages of all host galaxies used in cosmological analyses across the full redshift range and apply a relative age-bias correction to the SN distance modulus on a galaxy-by-galaxy basis. However, currently available host galaxy age measurements exist only for a limited number of samples at $z < 0.45$ (R19; Y. Kang et al. 2020; C. Chung et al. 2025), and therefore, such direct corrections cannot yet be applied to all host galaxies. Nevertheless, the evolution of the mean stellar population age within galaxies as a function of redshift can be inferred from the well-established cosmic star formation history (CSFH). The SN Ia progenitor age distribution (SPAD) can also be reliably obtained using the empirically derived SN Ia delay-time distribution (DTD) in conjunction with the CSFH (M. J. Childress et al. 2014).

In Fig. 2, following Y. Kang et al. (2020) and Y.-W. Lee et al. (2022), we adopt this method to estimate the redshift evolution of the SPAD. As shown by M. J. Childress et al. (2014), this result is not strongly affected by current uncertainties in the DTD. At low redshift,

[1]For other possible interpretations of the relative dimming of SNe at high redshift, the readers are referred to A. Aguirre & Z. Haiman (2000), A. K. Inoue & H. Kamaya (2004), and M. López-Corredoira & J. I. Calvo-Torel (2022).

the SPAD shows a distinct bimodality, with young (prompt) and old (delayed) components. At higher redshifts, however, the distribution becomes more uniform, dominated by the young population. Therefore, SN progenitors in host galaxies become progressively younger, on average, with increasing redshift, showing a similar trend to the evolution of the mean stellar population age derived from the CSFH. This prediction is well supported by directly measured ages from observational data for both SN Ia host galaxies and non-SN Ia host galaxies at present. Note that SN Ia arises in all types of galaxies and, thus, all galaxies were once SN Ia host galaxies. Therefore, SN Ia host galaxies in the sample used in the cosmological analysis – if we had measured population ages for all of them – would also follow the same redshift evolution of age predicted in Fig. 2. Assuming a linear relationship between host age and HR, we can thus apply a mean relative correction to the observed SN magnitude as a function of redshift, relative to $z = 0.0$. This relative average correction is obtained by multiplying the relative age difference by the slope of the age bias derived in Section 2:

$$\Delta m(z) = \Delta\mathrm{age}(z) \times 0.030\,\mathrm{mag\,Gyr^{-1}}. \quad (1)$$

As illustrated in the right panels of Fig. 2, within the redshift range most relevant to SN cosmology ($0 < z < 1$), we expect, on average, a 5.3 Gyr variation in progenitor age (top panel) and, therefore, a $\sim$0.16 mag variation in SN luminosity (bottom panel). This relative correction, $\Delta m(z)$, with respect to $z = 0.0$, is then integrated into the formula for the standardized distance modulus from SNe Ia:

$$\mu_{\mathrm{SN}} = m - M + \alpha x_1 - \beta c - \Delta m(z), \quad (2)$$

where m is the apparent magnitude, M is the absolute magnitude at the reference point ($x_1 = 0.0$, $c = 0.0$), x_1 and c are the light-curve width and colour parameters, and α and β are the absolute values of the slopes of the WLR and CLR, respectively. For the values of α and β, we adopt 0.148 and 3.09 for the Pantheon+ sample (D. Brout et al. 2022), and 0.161 and 3.12 for the 5 yr of the Dark Energy Survey Supernova (DES-SN5YR) data (DES Collaboration 2024). We apply this average correction to all SN data at each redshift. Although this approach does not reduce the scatter in HR values caused by variation in progenitor age at a given redshift, it does allow for an appropriate correction of the mean HR value in each redshift bin. Since cosmological parameters are mostly determined based on the average values of SN data within each redshift bin, applying a mean correction still allows us to predict the resulting changes in the cosmological model. While the result in Fig. 2 is derived under the flat w_0w_aCDM model using the cosmological parameters predicted from the DESI BAO Data Release 2 (DR2) combined with CMB data (table 5 of DESI Collaboration 2025), our corrections for the progenitor age bias in the cosmological analysis below are self-consistently determined with the cosmological fit.

Fig. 3 compares the binned SN data from the Dark Energy Survey (DES) project (DES Collaboration 2024) with cosmological models in the residual Hubble diagram, where HR $= \mu_{\mathrm{SN}} - \mu_{\mathrm{model}}$. Following DES Collaboration (2024), the H_0 and the SN Ia absolute magnitude M are combined in the single parameter $M + 5\log(c/H_0) = -11.80$. Therefore, the value of H_0 has no impact on the cosmological analysis. Before the age-bias correction, the SN data are broadly consistent with the ΛCDM model. After correcting for the age bias, however, the SN data set no longer supports the ΛCDM model. Instead, interestingly, it aligns more closely with a time-varying dark energy equation-of-state model (flat w_0w_aCDM), as recently suggested by the DESI BAO (DR2) project in a combined analysis of BAO and CMB (DESI Collaboration 2025). As compared in the top panel of Fig. 3, it is important to note that this model derived from BAO+CMB alone is even further away from the ΛCDM model than the w_0w_aCDM model most extensively discussed in the DESI papers, which is based on the combined analysis of BAO, CMB, and SNe before age-bias correction.

Within the same w_0w_aCDM model favoured by BAO+CMB, in Fig. 4, comparison is made between the SN and BAO distances in the residual Hubble diagram. The employed BAO distances are transverse comoving distances, $d_M(z)$, adopted from DESI Collaboration (2025). Additional BAO distance data are also adopted from DES Collaboration (2025). To directly compare with SN distances, these BAO distances are transformed to the luminosity distance via $d_L(z) = (1 + z)d_M(z)$. In order to be fully internally consistent, the value for the product of H_0 and the sound horizon (r_d) is also adopted from the same combined analysis of DESI BAO (DR2) and CMB in the w_0w_aCDM model (see Section 4.3; see also table 7 of DESI Collaboration 2025). Within this fixed value ($r_dh = 93.9 \pm 2.8$ Mpc), any combination of H_0 and r_d produces the same result. If the ΛCDM model had been assumed, the value of r_dh would increase and the BAO distances would shift closer to the ΛCDM prediction. However, given that the DESI project favours the w_0w_aCDM model, we consider it appropriate to adopt the r_dh value derived from this model. It is clear from Fig. 4 that, before the age-bias correction, the SN distances do not match with the BAO distances. After the correction, however, the SN distance scale matches very well with the BAO distance scale in the w_0w_aCDM model favoured by BAO+CMB. Therefore, the revised standard candle (SNe Ia) is in agreement with the standard ruler (BAO). For more detailed analysis and cosmological parameter estimation, following the DESI BAO papers (A. G. Adame et al. 2025; DESI Collaboration 2025), we have combined SN data set with BAO and CMB data in the flat w_0w_aCDM model, and compared that with the probability distribution for BAO combined only with CMB. The result of this analysis is presented in the following section.

4 COSMOLOGICAL ANALYSIS

4.1 Data sets and cosmological calculations

In this paper, we employ two different SN Ia data sets, the Pantheon+ sample (D. Brout et al. 2022) and the DES-SN5YR Data Release (DES Collaboration 2024). For the BAO measurements, we make use of the DESI BAO (DR2) data set (DESI Collaboration 2025). For the CMB analysis, multiple data sets are combined following the methodology described in the DESI DR2 paper. These include the SimAll and Commander likelihoods from the *Planck* PR3 (Public Release 3) release (Planck Collaboration V 2020), the CamSpec likelihood based on the *Planck* PR4 (Public Release 4) NPIPE maps (E. Rosenberg, S. Gratton & G. Efstathiou 2022), and the CMB lensing measurements from the *Planck* PR4 NPIPE release (J. Carron, M. Mirmelstein & A. Lewis 2022), together with the ACT DR6 (N. MacCrann et al. 2024; M. S. Madhavacheril et al. 2024; F. J. Qu et al. 2024). In the following sections, we refer to the DES-SN5YR data set as DES5Y, the Pantheon+ data set as Pantheon+ in the main text but abbreviated as 'Panth.' in tables and figures, the DESI DR2 data set as BAO, and the combined *Planck*+ACT data set as CMB.

We consider two cosmological models under the assumption of flat curvature: the wCDM model (see Section 4.2), where the dark energy equation-of-state parameter w is constant, and the w_0w_aCDM model (see Section 4.3), parametrized via the Chevallier–Polarski–Linder (CPL; M. Chevallier & D. Polarski 2001; E. V. Linder 2003) form, in which w evolves with time. Bayesian analysis of

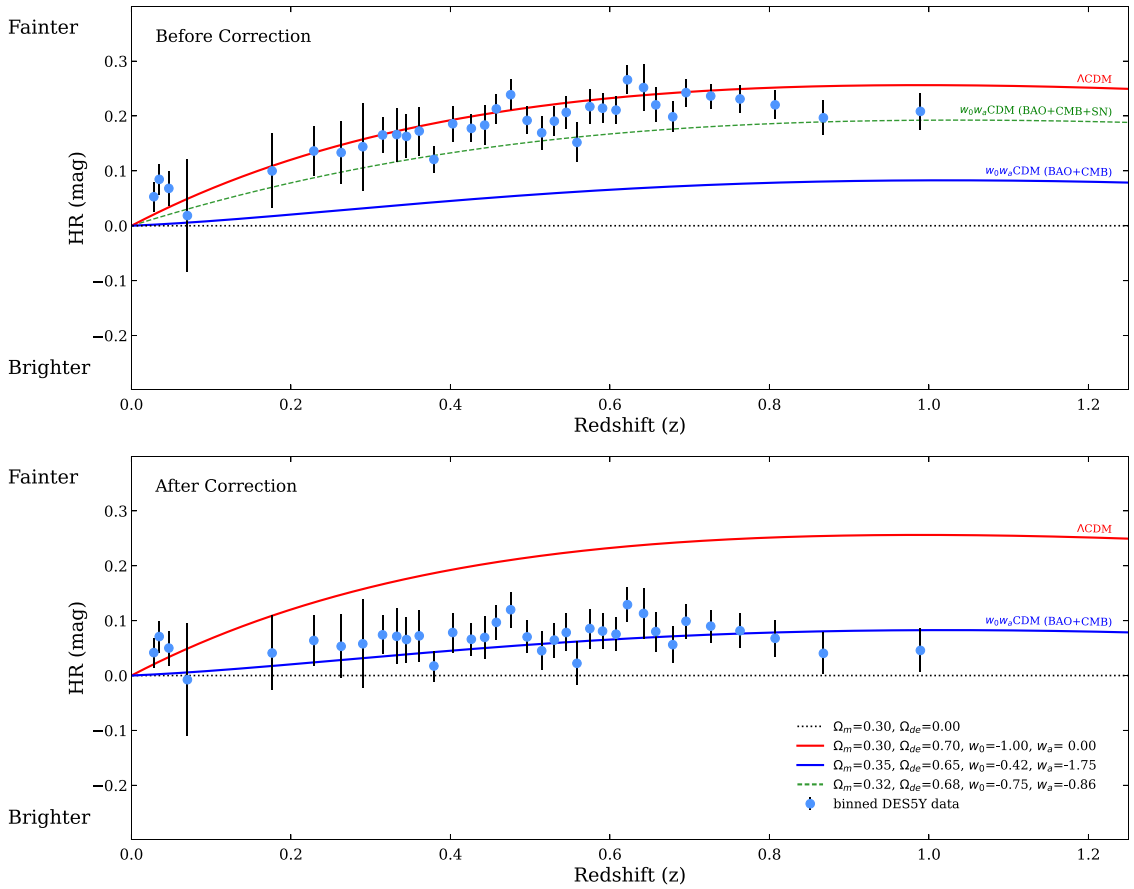

Figure 3. The residual Hubble diagram before (top panel) and after (bottom panel) the age-bias correction. The corrections are applied to the observational data from the DES SN project (DES Collaboration 2024), using the ΔHR/Δage slope (0.030 ± 0.004 mag Gyr^{-1}) and the redshift evolution of the median progenitor age relative to $z = 0.0$, as shown in Fig. 2. After the correction, the SN data set no longer supports the ΛCDM model (red solid lines), but instead shows better consistency with a time-varying dark energy equation of state, as described by the flat w_0w_aCDM model favoured by the combined BAO and CMB analysis (blue solid lines). As shown in the top panel, this model from BAO+CMB alone deviates significantly from that based on the combined analysis of BAO, CMB, and uncorrected SN data (green dashed line). In both cases, the relevant cosmological parameters are adopted from DESI Collaboration (2025). A binning scheme similar to that of the DES SN project was implemented to ensure ∼50 SNe per bin. In the bottom panel, an uncertainty in the age-bias slope was propagated into the total error budget of the binned data. A similar trend is also obtained when using the Pantheon+ data set (D. Brout et al. 2022).

the model parameters is performed via Markov chain Monte Carlo (MCMC) sampling (A. Lewis & S. Bridle 2002; R. M. Neal 2005; A. Lewis 2013) using COBAYA (J. Torrado & A. Lewis 2021), while cosmological calculations are carried out using the Boltzmann code CAMB (A. Lewis, A. Challinor & A. Lasenby 2000; C. Howlett et al. 2012). To evaluate the impact of the age-bias correction on the findings of DESI Collaboration (2025), we set our free parameters and priors as closely as possible to those used in their paper. For the analysis based solely on SN data, for consistency, we also adopt the same priors on Ω_m, w_0, and w_a as in DESI Collaboration (2025). As described in Section 3, SN-only result is not affected by the value of H_0 (see DES Collaboration 2024). As the age-bias correction is applied exclusively to the SN Ia data, our focus remains on the parameters Ω_m, w_0, and w_a, which are most directly constrained by SN Ia observations. We also report the present-day deceleration parameter, q_0, derived from w_0 and Ω_m, where a negative q_0 indicates an accelerating universe and a positive q_0 corresponds to a decelerating universe. Thus, we present four key parameters: Ω_m, w_0, w_a, and q_0. Parameter estimates, obtained with GETDIST (A. Lewis 2025), are presented as means with standard deviations for symmetric distributions or as means with 68 per cent credible intervals in other cases.

4.2 Flat wCDM model

The wCDM model extends the ΛCDM model by introducing the dark energy equation-of-state parameter w, which is assumed to be constant. In this subsection, we examine how the parameter estimates in the flat wCDM model are affected by applying the age-bias correction to the SN data. Fig. 5 shows constraints on Ω_m and w for the BAO, CMB, and DES5Y data sets. The left and right panels correspond to DES5Y data before and after the age-bias correction, respectively. Before the age-bias correction, the SN data yield $w = -0.82 \pm 0.15$. The CMB contours overlap only marginally with those from SNe and BAO, but a small overlapping region near $w = -1$ still supports the cosmological constant when all three probes are combined.

On the other hand, after applying the age-bias correction to the DES5Y data, the value of w increases to $w = -0.56^{+0.18}_{-0.08}$. Now the SN contours deviate from those of the BAO and CMB by more

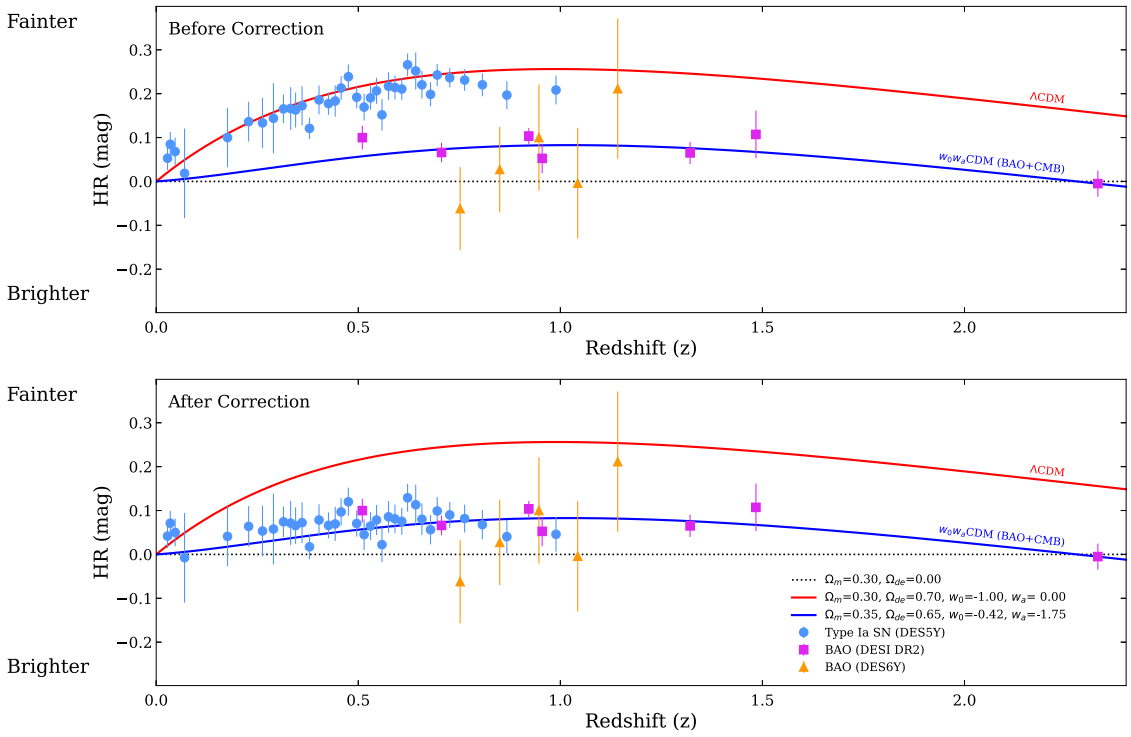

Figure 4. Similar to Fig. 3, but showing the comparison between SN and BAO distance measurements. The BAO distances are taken from DESI Collaboration (2025, DESI DR2 shown in magenta squares) and DES Collaboration (2025, DES6Y shown in orange triangles) and have been converted to distance moduli. After correcting for the progenitor age bias (bottom panel), the SN and BAO distance scales show good agreement. For a self-consistent comparison, we adopt the value of the product $H_0\, r_d$ from the combined DESI BAO (DR2) and CMB analysis within the flat w_0w_aCDM model (see text for details).

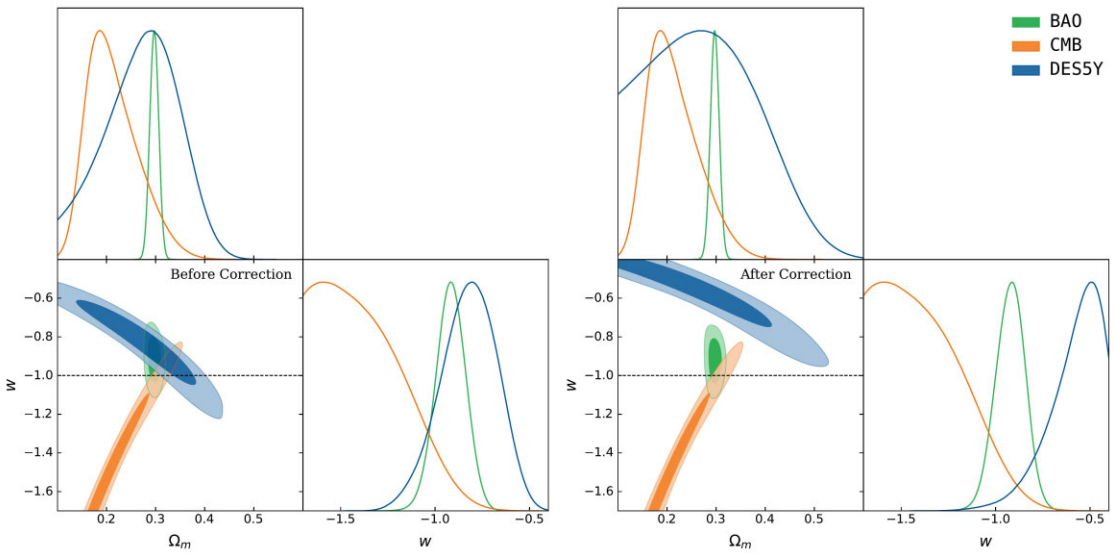

Figure 5. Confidence contours (68 per cent and 95 per cent) in the Ω_m–w plane for the flat wCDM model. The DES5Y SN data, shown before and after the age-bias correction (left and right panels, respectively), are compared with BAO and CMB data. In the left panel, a small overlap near $w = -1$ weakly supports the ΛCDM model when all three data sets are combined. In the right panel, after applying the age-bias correction, the SN contours shift upward, favouring a significantly larger value of w ($\sim$−0.56). The three probes no longer intersect near $w = -1$, but instead show a progression in the mean w values: from the CMB ($w \approx -1.5$, $z \approx 1090$), to BAO ($w \sim -0.92$, $0.4 < z < 4$), and to SNe Ia ($w \sim -0.56$, $0 < z < 1.5$), suggesting a redshift evolution of the dark energy equation-of-state parameter.

Table 1. Cosmological parameter constraints in the flat wCDM model. Parameter estimates are presented as means with standard deviations for approximately symmetric posterior distributions, or as means with 68 per cent credible intervals for non-Gaussian cases. Results are shown for individual data sets – BAO only, CMB only, and SN only – both before and after the age-bias correction applied to the SN data.

Data set	Ω_m	w	q_0
BAO	0.297 ± 0.009	-0.917 ± 0.078	-0.467 ± 0.082
CMB	$0.211^{+0.023}_{-0.068}$	-1.491 ± 0.272	-1.285 ± 0.426
Panth.	0.277 ± 0.073	-0.894 ± 0.148	-0.455 ± 0.071
DES5Y	0.265 ± 0.083	-0.821 ± 0.149	-0.388 ± 0.071
Panth. (corrected)	0.252 ± 0.117	$-0.595^{+0.176}_{-0.094}$	$-0.143^{+0.064}_{-0.044}$
DES5Y (corrected)	0.247 ± 0.125	$-0.556^{+0.181}_{-0.078}$	$-0.102^{+0.066}_{-0.042}$

than 2σ in the w–Ω_m plane, breaking the previous concordance and revealing significant tension among the data sets. Table 1 presents the estimated values of Ω_m, w, and q_0 for the BAO, CMB, and SN data sets, including the Pantheon+. As shown in the table, the Pantheon+ exhibit a similar increase in w after the age-bias correction. An interesting trend is observed among three probes at different cosmic epochs. The CMB, a high-redshift ($z \sim 1090$) probe, yields the lowest w value ($w = -1.5$), whereas the BAO, an intermediate-redshift ($0.4 < z \lesssim 4$) probe, tends to produce an intermediate w value ($w = -0.92$). After the age-bias correction, the SN data, covering the lowest redshift range ($0 < z \lesssim 1.5$), exhibit $w \sim -0.6$, the highest w value among all probes considered. The w values inferred from different probes exhibit a monotonic increase with decreasing redshift, suggesting a redshift-dependent evolution of the dark energy equation of state. This observed trend provides a compelling motivation to investigate the dynamical dark energy model in the following subsection.

4.3 Flat w_0w_aCDM model: a new concordance

The CPL parametrization, expressed as $w(a) = w_0 + w_a(1 - a)$, provides the simplest framework for describing dynamical dark energy. Here, w_0 represents the present-day value of the dark energy equation of state, while w_a quantifies its variation with respect to the scale factor. Motivated by the findings of the A. G. Adame et al. (2025) and DESI Collaboration (2025), we analyse the behaviour of the constrained parameters w_0, w_a, and q_0 within the CPL parametrization when the age-bias correction is applied to SN Ia data.

Fig. 6 illustrates the effect of age-bias correction on the two SN data sets in combination with the BAO data. The BAO-only contour (grey) provides a reference for comparing the shift in the BAO+SNe contours before and after age-bias correction. The BAO data alone yield $w_0 = -0.47^{+0.34}_{-0.18}$ and $w_a = -1.69^{+0.46}_{-1.23}$, indicating a mild deviation from the ΛCDM values, consistent with DESI Collaboration (2025). The mean value of q_0 based on the BAO data is greater than zero ($q_0 = 0.028^{+0.36}_{-0.17}$), with the distribution showing no preference for an accelerating universe. For the SN-only analysis using the DES5Y sample, the estimated parameters, before the age-bias correction, are $w_0 = -0.82 \pm 0.13$, $w_a = -1.77^{+0.43}_{-1.21}$, and $q_0 = -0.26^{+0.12}_{-0.10}$. After the age-bias correction, these values shift to $w_0 = -0.56^{+0.15}_{-0.12}$, $w_a = -1.75^{+0.47}_{-1.22}$, and $q_0 = 0.028 \pm 0.10$. A

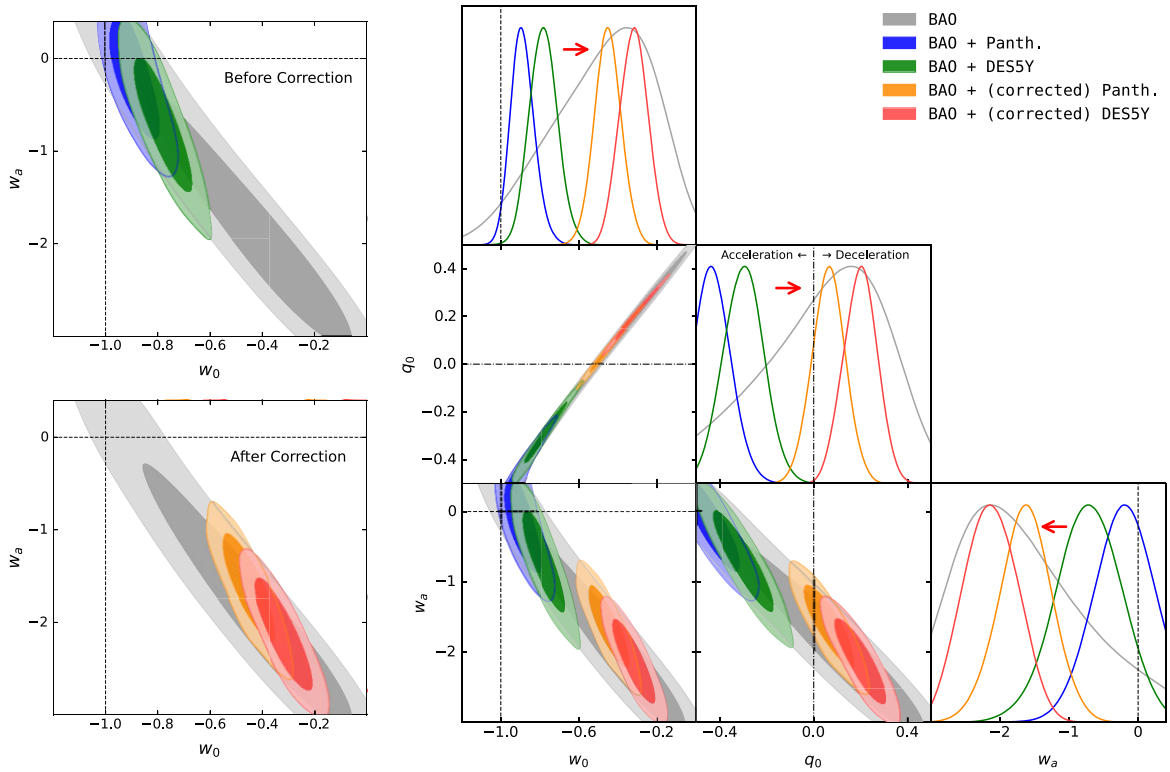

Figure 6. Posterior distributions in the w_0–w_a, w_0–q_0, and q_0–w_a parameter spaces for the flat w_0w_aCDM model. The contours represent 68 per cent and 95 per cent credible intervals, derived from BAO alone (grey) and BAO combined with Pantheon+ or DES5Y SN data sets before (blue and green) and after (orange and red) the age-bias correction. After applying the age-bias correction, the combined (BAO+SNe) constraints become more consistent with the BAO-only results.

Table 2. Cosmological parameter constraints in the flat w_0w_aCDM model. As in Table 1, parameter estimates are presented either as means with standard deviations or as means with 68 per cent credible intervals. The results are distinguished by whether or not CMB data are included. For each combination, results are shown both before and after applying the age-bias correction to the SN data, with the corrected cases explicitly labelled.

Data set	Ω_m	w_0	w_a	q_0
BAO	$0.353^{+0.040}_{-0.020}$	$-0.473^{+0.336}_{-0.184}$	$-1.687^{+0.463}_{-1.234}$	$0.028^{+0.361}_{-0.168}$
Panth.	0.319 ± 0.095	-0.923 ± 0.147	-0.634 ± 1.015	-0.428 ± 0.102
DES5Y	$0.376^{+0.069}_{-0.025}$	-0.820 ± 0.131	$-1.771^{+0.425}_{-1.206}$	$-0.261^{+0.118}_{-0.096}$
Panth. (corrected)	0.360 ± 0.127	$-0.652^{+0.187}_{-0.132}$	-0.842 ± 0.908	-0.104 ± 0.091
DES5Y (corrected)	$0.427^{+0.103}_{-0.035}$	$-0.562^{+0.151}_{-0.120}$	$-1.748^{+0.472}_{-1.216}$	0.028 ± 0.096
BAO+Panth.	$0.301^{+0.022}_{-0.011}$	-0.889 ± 0.060	-0.196 ± 0.437	-0.433 ± 0.078
BAO+DES5Y	$0.319^{+0.017}_{-0.011}$	-0.782 ± 0.071	-0.713 ± 0.474	-0.300 ± 0.086
BAO+Panth. (corrected)	0.359 ± 0.011	-0.453 ± 0.068	-1.633 ± 0.381	0.064 ± 0.070
BAO+DES5Y (corrected)	0.374 ± 0.011	-0.320 ± 0.072	-2.136 ± 0.386	0.199 ± 0.070
CMB data included				
BAO+CMB	0.352 ± 0.021	-0.430 ± 0.207	-1.704 ± 0.580	0.075 ± 0.215
BAO+CMB+Panth.	0.311 ± 0.006	-0.838 ± 0.054	-0.612 ± 0.201	-0.366 ± 0.061
BAO+CMB+DES5Y	0.319 ± 0.006	-0.754 ± 0.056	-0.848 ± 0.217	-0.271 ± 0.061
BAO+CMB+Panth. (corrected)	0.353 ± 0.006	-0.447 ± 0.059	-1.585 ± 0.227	0.065 ± 0.060
BAO+CMB+DES5Y (corrected)	0.363 ± 0.006	-0.337 ± 0.062	-1.902 ± 0.246	0.178 ± 0.061

similar trend is observed in the Pantheon+ data set (see Table 2). Before the age-bias correction, the estimated parameters for the combination of BAO and the Pantheon+ SN data set are

$$\left.\begin{aligned} w_0 &= -0.89 \pm 0.06 \\ w_a &= -0.20 \pm 0.44 \\ q_0 &= -0.43 \pm 0.08 \end{aligned}\right\} \quad \text{BAO+Panth.,}$$

and for the combination with DES5Y, they become

$$\left.\begin{aligned} w_0 &= -0.78 \pm 0.07 \\ w_a &= -0.71 \pm 0.47 \\ q_0 &= -0.30 \pm 0.09 \end{aligned}\right\} \quad \text{BAO+DES5Y.}$$

These values are almost identical to those reported in DESI Collaboration (2025). When combined with BAO measurements, the SN data before the age-bias correction reduce the apparent deviation from ΛCDM cosmology observed in BAO-only analyses. The inclusion of SN data without age-bias correction shifts the best-fitting values of the dark energy parameters closer to those predicted by the ΛCDM model. Furthermore, the resulting deceleration parameter q_0 becomes clearly negative, favouring an accelerating universe.

After the age-bias correction, however, the estimated values are substantially changed. For the combination with the corrected Pantheon+, they become

$$\left.\begin{aligned} w_0 &= -0.45 \pm 0.07 \\ w_a &= -1.63 \pm 0.38 \\ q_0 &= 0.064 \pm 0.070 \end{aligned}\right\} \quad \text{BAO+Panth. (corrected),}$$

and for the combination with the corrected DES5Y, they are changed to

$$\left.\begin{aligned} w_0 &= -0.32 \pm 0.07 \\ w_a &= -2.14 \pm 0.39 \\ q_0 &= 0.199 \pm 0.070 \end{aligned}\right\} \quad \text{BAO+DES5Y (corrected).}$$

The addition of SN data, after applying the age-bias correction, supports the deviation from the ΛCDM model indicated by BAO-only measurements, yielding best-fitting values that are well aligned with the BAO-only case but with reduced uncertainties. The tension with the ΛCDM model exceeds 6σ for the BAO+DES5Y combination. Table 2 summarizes the estimated cosmological parameters, allowing a detailed comparison among BAO-only, SN-only, and BAO+SNe combinations with and without age-bias correction. For the combined data sets of both Pantheon+ and DES5Y, the application of the age-bias correction leads to a significant increase in w_0, consistent with the trend observed in the wCDM model, along with a substantial decrease in w_a, suggesting a stronger preference for a time-varying dark energy component. The correction also results in a marked increase in q_0, indicating a shift toward a non-accelerating universe.

Correcting for the age bias in SN data resulted in a notable discordance among cosmological probes in both the standard ΛCDM and flat wCDM models (see Y.-W. Lee et al. 2022 and Section 4.2). However, in a time-varying dark energy model, a new concordance emerges between BAO and SNe after the age-bias correction. To quantify the concordance among data sets, we compute the Kullback–Leibler (KL) divergence (S. Kullback & R. A. Leibler 1951). This metric is well suited for our analysis, since cosmological parameter posteriors are often strongly non-Gaussian and influenced by priors, making traditional comparisons based on means or standard deviations unreliable. The KL divergence, as presented in L. Verde, P. Protopapas & R. Jimenez (2013), is given by

$$D_{\rm KL}(\mathcal{P}\|\mathcal{W}) = \int_x \log_2\left(\frac{\mathcal{P}(x)}{\mathcal{W}(x)}\right)\mathcal{P}(x)\,{\rm d}x,$$

where $\mathcal{P}$ is the distribution of interest, and $\mathcal{W}$ is the reference distribution. A larger KL divergence indicates a greater difference between $\mathcal{P}$ and $\mathcal{W}$, with $D_{\rm KL} = 0$ indicating identical $\mathcal{P}$ and $\mathcal{W}$. In the upper panels of Fig. 7, we show the results of the KL divergence, calculated from the marginalized posterior distributions of the parameters, with the BAO-only data serving as a reference. The combination with the Pantheon+ SN data is shown in the left panel, and that with the DES5Y SN data in the right panel. For all relevant parameters, the BAO+SNe combination exhibits lower KL divergences after applying the age-bias correction, indicating improved consistency with the BAO-only constraints.

This trend not only persists but becomes more pronounced when CMB data are combined with BAO and SN probes. Fig. 8 illustrates the impact of the age-bias correction on cosmological inferences derived from the combined BAO+CMB+SN data sets.

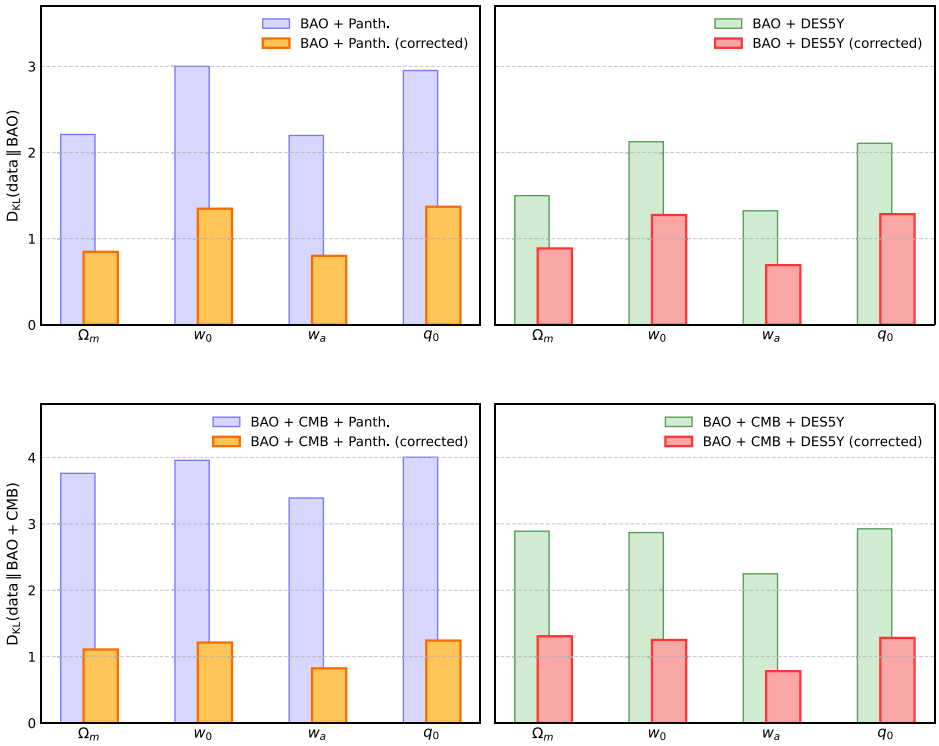

Figure 7. Results of the KL divergence analysis. The SN data sets are Pantheon+ (left) and DES5Y (right). The upper panels show the KL divergence of marginalized cosmological parameter posteriors, using BAO data alone as the reference. In both cases, the BAO+SNe combinations exhibit lower KL divergence after the age-bias correction, indicating improved consistency with the BAO-only results. The lower panels display the KL divergence relative to the BAO+CMB combination. Again, the application of the age-bias correction consistently reduces the KL divergence for all parameters, indicating improved agreement between the SN-added results (BAO+CMB+SN) and the BAO+CMB.

The parameter estimates are also summarized in Table 2. The combined analysis is categorized by the SN sample used (Pantheon+ or DES5Y) and by whether the age-bias correction is applied. The BAO+CMB only contours (grey) serve as a reference, highlighting changes in the posterior distributions resulting from the application of age-bias correction. It is important to note that the BAO+CMB only combination already suggests best-fitting parameters ($w_0 = -0.43 \pm 0.21$, $w_a = -1.70 \pm 0.58$, and $q_0 = 0.075 \pm 0.215$) that significantly deviate from ΛCDM at the $\sim 3.0\sigma$ level, which is almost identical to the result from DESI DR2 (3.1σ). Our analysis indicates that these values have not changed much since the Sloan Digital Sky Survey BAO (S. Alam et al. 2021) and DESI DR1 results, although the associated uncertainties have been reduced. However, when the SN data set before the age-bias correction is added here, the resulting SN-added contours lie closer to ΛCDM for both Pantheon+ and DES5Y. The estimated parameters for the combination with the Pantheon+ are

$$\left.\begin{aligned} w_0 &= -0.84 \pm 0.05 \\ w_a &= -0.61 \pm 0.20 \\ q_0 &= -0.37 \pm 0.06 \end{aligned}\right\} \quad \text{BAO+CMB+Panth.,}$$

and for the combination with DES5Y, they become

$$\left.\begin{aligned} w_0 &= -0.75 \pm 0.06 \\ w_a &= -0.85 \pm 0.22 \\ q_0 &= -0.27 \pm 0.06 \end{aligned}\right\} \quad \text{BAO+CMB+DES5Y.}$$

These values are fully consistent with those in table 5 of DESI Collaboration (2025). Although the SN-added contours deviate from ΛCDM by 3.1σ (Pantheon+) and 4.4σ (DES5Y), as measured by the Mahalanobis distance in the (w_0, w_a) parameter space, they do not lie near the peak of the posterior distribution predicted solely from the BAO+CMB. Instead, they are located near the edge of the distribution, indicating a discordance between the BAO+CMB and the SN data before the age-bias correction. The SN data set pulls the mean values of the dark energy equation-of-state parameters closer to the ΛCDM model.

However, after correcting the SN data for progenitor age bias, the SN-added results shift back toward the BAO+CMB-only contours, aligning more closely with them for both the Pantheon+ and DES5Y samples. When the corrected Pantheon+ SN sample is combined with BAO+CMB, the best-fitting values of w_0, w_a, and q_0 are

$$\left.\begin{aligned} w_0 &= -0.45 \pm 0.06 \\ w_a &= -1.59 \pm 0.23 \\ q_0 &= 0.065 \pm 0.060 \end{aligned}\right\} \quad \text{BAO+CMB+Panth. (corrected),}$$

and when the corrected DES5Y SN sample is added, they become

$$\left.\begin{aligned} w_0 &= -0.34 \pm 0.06 \\ w_a &= -1.90 \pm 0.25 \\ q_0 &= 0.178 \pm 0.061 \end{aligned}\right\} \quad \text{BAO+CMB+DES5Y (corrected).}$$

The right panels of Fig. 8 show that the posterior distributions for w_0, w_a, and q_0, all agree more closely with those from BAO+CMB alone after applying the age-bias correction. The KL divergence, computed using the BAO+CMB-only combination as the reference

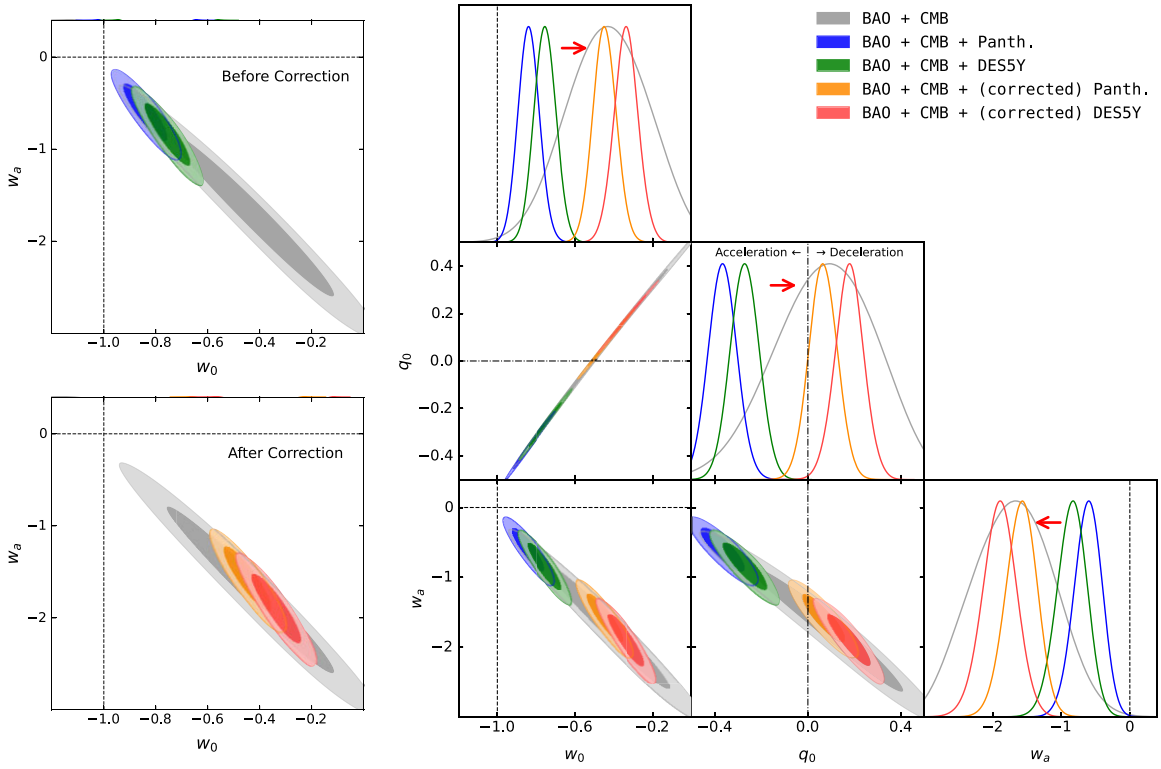

Figure 8. Same as Fig. 6, but with CMB data included in the analysis. The contours are derived from the combination of BAO+CMB (grey), and BAO+CMB combined with each of the Pantheon+ and DES5Y SN Ia data sets before (blue and green) and after (orange and red) the age-bias correction, respectively. After applying the age-bias correction, the SN-added results (BAO+CMB+SNe) align more closely with the BAO+CMB posteriors across all three parameters (w_0, w_a, q_0).

(see the bottom panels of Fig. 7), also decreases consistently across all relevant parameters when the age-bias correction is applied, indicating improved agreement among the probes. Thus, a new cosmological concordance emerges when the SN distance scale is corrected for age bias within the w_0w_aCDM model. The discordance with the ΛCDM model now reaches at 9.8σ (Pantheon+) and 11.7σ (DES5Y), as quantified by the Mahalanobis distance in the (w_0, w_a) parameter space, strongly suggesting a time-varying dark energy equation of state.

The SN data sets used in our analysis, DES5Y and Pantheon+, incorporate the host galaxy stellar mass-step correction in SN magnitude standardization. This is a magnitude offset between hosts above and below $\sim 10^{10}\,M_\odot$, commonly parametrized by γ. As discussed in Section 2, the mass-step correction cannot account for the redshift-dependent bias arising from progenitor age, as the evolution of progenitor age with redshift differs significantly from that of host galaxy mass. Nevertheless, it is important to assess the potential for overcorrection when both the age-bias and host-mass corrections are applied to SN magnitudes. We therefore performed this test using the DES5Y data set, which adopts $\gamma = 0.038$. For the Pantheon+, the γ value is apparently negligible, with $\gamma = -0.003$. In the w_0w_aCDM model using only the SN data set, removing the host mass-step correction (i.e. $\gamma = 0$) shifts the best-fitting parameters by $\Delta w_0 = -0.036$, $\Delta w_a = 0.016$, and $\Delta q_0 = -0.015$. When BAO and CMB data are included, the corresponding shifts are $\Delta w_0 = 0.002$, $\Delta w_a = 0.005$, and $\Delta q_0 = 0.003$. Overall, the impact of the host mass-step correction on our results is negligible relative to the impact of the age-bias correction and the typical MCMC posterior uncertainties.

5 DISCUSSION

Our analysis is fundamentally different from previous studies that incorporated progenitor age effects only indirectly through age proxies. For example, M. Rigault et al. (2020) and N. Nicolas et al. (2021), using the SN magnitude step with the local specific star formation rate, considered only the redshift evolution of the relative fractions of 'young' and 'old' progenitors, without accounting for the absolute age evolution of the 'old' progenitors across redshift. As shown in Fig. 2, the mean age of 'old' progenitors declines markedly from ∼10 to ∼3 Gyr between $z = 0.0$ and $z = 1.0$. This systematic effect was not included in their analyses, leading to a significant underestimation of the full impact of progenitor age bias. The DES SN program, as described by M. Vincenzi et al. (2024), employed the progenitor age model of P. Wiseman et al. (2021) solely to explore the correlation between the light-curve width parameter x_1 and progenitor age. However, this limited treatment was incorporated only into the systematic error budget, with its impact reportedly negligible (see their table 7). The direct correlation between host age and HR, together with the redshift evolution of the mean progenitor age, as described in Sections 2 and 3, has not been explicitly incorporated into SN cosmology analyses by other studies.

The most intriguing outcome of our study is that it offers a new perspective on the evolution of the deceleration parameter. Fig. 9 illustrates how the deceleration parameter evolves over time, before and after applying the progenitor age-bias correction to the SN data. For comparison, it also shows the evolution predicted by the ΛCDM model, which has been the standard cosmological model until

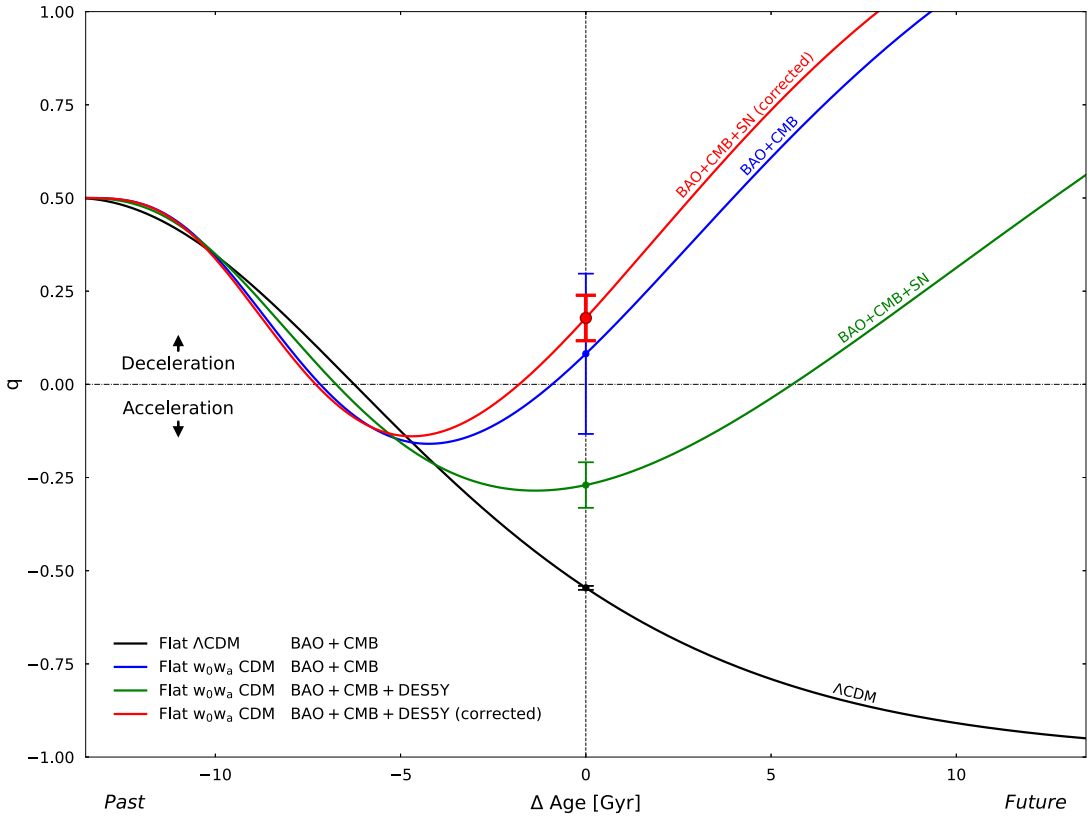

Figure 9. Evolution of the deceleration parameter, $q = -\ddot{a}a/\dot{a}^2$, of the universe. The vertical dotted line indicates the present age of the universe. The black line shows the result from the BAO+CMB data under the assumption of the flat ΛCDM model. The green and red lines represent the flat w_0w_aCDM models derived from the combined data sets (BAO+CMB+DES5Y SN) before and after applying the age-bias correction to the SN data set, respectively. After the age-bias correction, the combined data sets suggest that the universe is already in a state of decelerated expansion ($q_0 > 0$) at the present epoch (Δage = 0.0 Gyr) and will remain so in the future, consistent with the prediction from DESI BAO combined with CMB alone (the blue line).

recently. As is well known, the ΛCDM model predicts that the present universe is in a phase of accelerated expansion and will continue to accelerate in the future. In contrast, the evolution predicted when the DESI BAO result is combined with CMB and SN data shows that the future universe will transition to a state of decelerated expansion. Nevertheless, even in this case, the present universe remains in a phase of accelerated expansion ($q_0 < 0$). However, when the progenitor age-bias correction is applied to the SN data, not only does the future universe transition to a state of decelerated expansion, but the present universe also already shifts toward a state closer to deceleration rather than acceleration. Interestingly, this result is consistent with the prediction obtained when only the DESI BAO and CMB data are combined, as discussed in Section 1. Together with the DESI BAO result, which suggests that dark energy may no longer be a cosmological constant, our analysis raises the possibility that the present universe is no longer in a state of accelerated expansion. This provides a fundamentally new perspective that challenges the two central pillars of the ΛCDM standard cosmological model proposed 27 yr ago.

The progenitor age bias in SN cosmology might also contribute to alleviating the Hubble tension (A. G. Riess et al. 2022). This arises from the potential population mismatch between the host galaxies in the calibration sample and those in the Hubble flow sample. Currently, the calibrating galaxies in the second rung of the distance ladder are all late-type galaxies with relatively young stellar populations, whereas host galaxies in the Hubble flow sample (third rung) generally encompass all morphological types and, on average, have relatively older stellar populations (A. G. Riess et al. 2011; W. L. Freedman 2021). More recently, A. G. Riess et al. (2022) argue that they employ only spiral galaxies for the Hubble flow sample to minimize this potential population mismatch. However, simply selecting host galaxies based on morphological classification may not sufficiently ensure that the SNe Ia in the third rung are identical to those in the second rung in terms of progenitor age. This is particularly relevant because M. Rigault et al. (2015) demonstrated that most SNe Ia in the second rung originate from locally star-forming environments, whereas, according to L. S. Aramyan et al. (2016), only two-thirds of spiral galaxies host SNe Ia on spiral arms (i.e. in locally star-forming, young environments). Therefore, if the conclusion of M. Rigault et al. (2015) remains valid for the expanded sample of 37 late-type calibrating galaxies in A. G. Riess et al. (2022), we would still expect some population mismatch between the SNe Ia in the second and third rungs. Furthermore, the accuracy of morphological classification is not complete and estimated to be ∼90 per cent at $z \sim 0.1$ (C. Park & Y.-Y. Choi 2005), and, therefore, not all of the Hubble flow sample in A. G. Riess et al. (2022) would be purely spiral hosts. Taken together, only ∼60 per cent of SNe Ia in the Hubble flow sample of A. G. Riess et al. (2022) might originate from relatively young populations, whereas ∼90 per cent of SNe Ia in the calibration sample could be from such populations. The extreme case of the age bias in the Hubble tension is expected between the calibration sample (mostly late-type galaxies) and the host galaxies

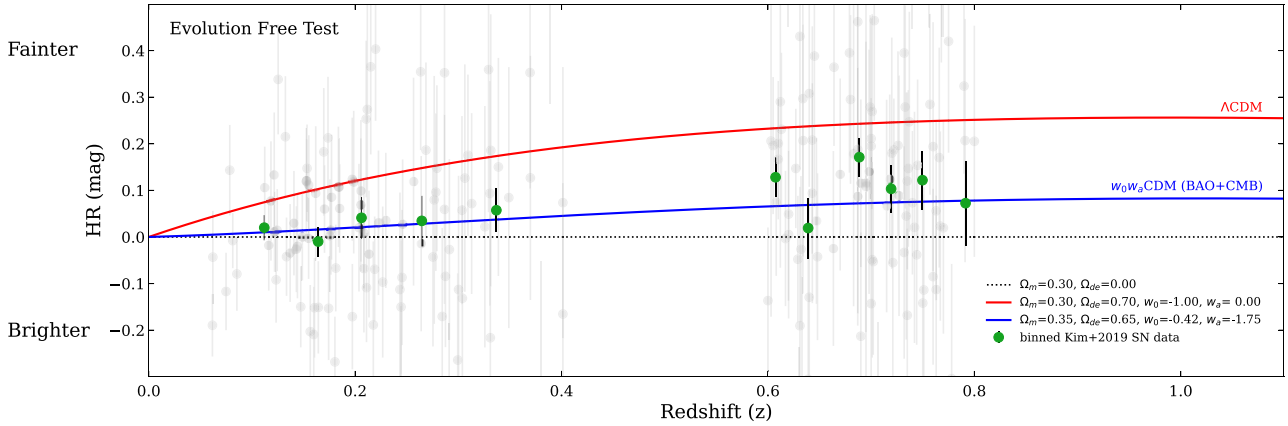

Figure 10. The evolution-free cosmological test in the residual Hubble diagram. Only SNe from young (<4.5 Gyr) host galaxies are selected from the R19 and G11 samples at $0.05 < z < 0.4$, such that their mean stellar population age (3.1 Gyr) matches that of host galaxies at $z = 0.7 \pm 0.1$. The HR values are taken from Y.-L. Kim et al. (2019) with a 0.146 mag offset applied to account for the mean age difference between all host galaxies and the young hosts at $z \sim 0.0$ (grey open circles). The binned SN data (green circles) are more consistent with the w_0w_aCDM model favoured by DESI BAO (DR2) and CMB combination (blue line) than with the ΛCDM model (red line).

in the Coma Cluster, which comprises mostly early-type galaxies. Indeed, a recent study by D. Scolnic et al. (2025) indicates that the Hubble tension is becoming even more severe in this case. If this possibility is confirmed by direct age measurements of stellar populations in host galaxies, even a 2–3 Gyr difference in the average age between the second and third rungs could significantly reduce (by 3–4.5 per cent, $\Delta H_0 = 2.2$–3.3 km s^{-1} Mpc^{-1}) the value of the Hubble constant while increasing its systematic error. This, in turn, could substantially alleviate the Hubble tension.

The redshift-dependent age-bias correction applied in this study is in good agreement with the directly observed evolution of the mean stellar population age of galaxies (see Fig. 2). Therefore, on average, this approach appropriately accounts for the systematic variation of the age bias with redshift. To provide a more direct cosmological analysis free from the need for progenitor age-bias correction, we also perform an 'evolution-free' cosmological test, where only SNe from young and coeval host galaxies are used across the full redshift range. This approach, suggested by several earlier studies (A. G. Riess et al. 1998; Y. Kang et al. 2016), yields cosmological constraints that are inherently free from the influence of the progenitor age bias. Fig. 10 presents the first result from this test. To maximize the number of host galaxies within a consistent SN catalogue, the HR values are taken from Y.-L. Kim, Y. Kang & Y.-W. Lee (2019), in which the mass-step correction is not applied. Based on the CSFH and direct age measurements of galaxies (Fig. 2), the mean stellar population age of SN host galaxies at $z = 0.7$ is estimated to be approximately 3.1 Gyr. We therefore select only comparably young (<4.5 Gyr) host galaxies at relatively low redshifts from the R19 and G11 samples that overlap with Y.-L. Kim et al. (2019) catalogue, such that their mean age also becomes 3.1 Gyr. As a result, the binned SN data in Fig. 10 represent a sample with approximately coeval progenitor ages across redshift. It is important to confirm that these homogeneous data remain more consistent with the w_0w_aCDM model preferred by the combined DESI BAO and CMB analysis than with the ΛCDM model. Fig. 10 therefore provides independent support that strengthens the overall conclusion of this study. In future work, we plan to extend this evolution-free test by measuring stellar population ages for additional host galaxies in currently undersampled redshift ranges.

ACKNOWLEDGEMENTS

We acknowledge support from the National Research Foundation of Korea to the Center for Galaxy Evolution Research (RS-2022-NR070872, RS-2022-NR070525).

DATA AVAILABILITY

This article makes use of BAO, CMB, and SN data that are publicly available at https://github.com/CobayaSampler. ACT DR6 data can be accessed at https://github.com/ACTCollaboration/act_dr6_lenslike. Hubble residuals of the YONSEI SN catalogue of Y.-L. Kim et al. (2019) were obtained through private communication with Young-Lo Kim. The ages of the corresponding SN Ia host galaxies are available at https://academic.oup.com/mnras/article/538/4/3340/8098234.

REFERENCES

Adame A. G. et al., 2025, J. Cosmol. Astropart. Phys., 02, 021
Aguirre A., Haiman Z., 2000, ApJ, 532, 28
Alam S. et al., 2021, Phys. Rev. D, 103, 083533
Aramyan L. S. et al., 2016, MNRAS, 459, 3130
Bell J. B., Day M. S., Rendleman C. A., Woosley S. E., Zingale M., 2004, ApJ, 606, 1029
Brout D., Scolnic D., 2021, ApJ, 909, 26
Brout D. et al., 2022, ApJ, 938, 110
Carron J., Mirmelstein M., Lewis A., 2022, J. Cosmol. Astropart. Phys., 09, 039
Chevallier M., Polarski D., 2001, Int. J. Mod. Phys. D, 10, 213
Childress M. J., Wolf C., Zahid H. J., 2014, MNRAS, 445, 1898
Chung C., Yoon S.-J., Park S., An S., Son J., Cho H., Lee Y.-W., 2023, ApJ, 959, 94
Chung C., Park S., Son J., Cho H., Lee Y.-W., 2025, MNRAS, 538, 3340
Conroy C., Gunn J. E., 2010, ApJ, 712, 833
Conroy C., Ho S., White M., 2007, MNRAS, 379, 1491
DES Collaboration, 2024, ApJ, 973, L14
DES Collaboration, 2025, preprint (arXiv:2503.06712)
DESI Collaboration, 2025, preprint (arXiv:2503.14738)
Freedman W. L., 2021, ApJ, 919, 16
Gallagher J. S., Garnavich P. M., Caldwell N., Kirshner R. P., Jha S. W.,Li W., Ganeshalingam M., Filippenko A. V. , 2008, ApJ, 685, 752

Gupta R. R. et al., 2011, ApJ, 740, 92 (G11)
Howlett C., Lewis A., Hall A., Challinor A., 2012, J. Cosmol. Astropart. Phys., 04, 027
Inoue A. K., Kamaya H., 2004, MNRAS, 350, 729
Jha S. W., Maguire K., Sullivan M., 2019, Nat. Astron., 3, 706
Johansson J. et al., 2013, MNRAS, 435, 1680
Kang Y., Kim Y.-L., Lim D., Chung C., Lee Y.-W., 2016, ApJS, 223, 7
Kang Y., Lee Y.-W., Kim Y.-L., Chung C., Ree C. H., 2020, ApJ, 889, 8
Kelly P. L., Hicken M., Burke D. L., Mandel K. S., Kirshner R. P., 2010, ApJ, 715, 743
Kim Y.-L., Kang Y., Lee Y.-W., 2019, J. Korean Astron. Soc., 52, 181
Kullback S., Leibler R. A., 1951, Ann. Math. Stat., 22, 79
Lee Y.-W., Chung C., Kang Y., Jee M. J., 2020, ApJ, 903, 22
Lee Y.-W., Chung C., Demarque P., Park S., Son J., Kang Y., 2022, MNRAS, 517, 2697
Lewis A., 2013, Phys. Rev. D, 87, 103529
Lewis A., 2025, J. Cosmol. Astropart. Phys., 08, 025
Lewis A., Bridle S., 2002, Phys. Rev. D, 66, 103511
Lewis A., Challinor A., Lasenby A., 2000, ApJ, 538, 473
Linder E. V., 2003, Phys. Rev. Lett., 90, 091301
López-Corredoira M., Calvo-Torel J. I., 2022, Int. J. Mod. Phys. D, 31, 2250104
MacCrann N. et al., 2024, ApJ, 966, 138
Madhavacheril M. S. et al., 2024, ApJ, 962, 113
Neal R. M., 2005, preprint (arXiv:math/0502099)
Nicolas N. et al., 2021, A&A, 649, A74
Pan Y. C. et al., 2014, MNRAS, 438, 1391
Park C., Choi Y.-Y., 2005, ApJ, 635, L29
Perlmutter S. et al., 1999, ApJ, 517, 565
Phillips M. M., 1993, ApJ, 413, L105
Planck Collaboration V, 2020, A&A, 641, A5
Planck Collaboration VI, 2021, A&A, 652, C4
Qu F. J. et al., 2024, ApJ, 962, 112
Riess A. G. et al., 1998, AJ, 116, 1009
Riess A. G. et al., 2011, ApJ, 730, 119
Riess A. G. et al., 2022, ApJ, 934, L7
Rigault M. et al., 2015, ApJ, 802, 20
Rigault M. et al., 2020, A&A, 644, A176
Rose B. M., Garnavich P. M., Berg M. A., 2019, ApJ, 874, 32 (R19)
Rosenberg E., Gratton S., Efstathiou G., 2022, MNRAS, 517, 4620
Rubin D. et al., 2025, ApJ, 986, 231
Schmidt B. P. et al., 1998, ApJ, 507, 46
Scolnic D. et al., 2025, ApJ, 979, L9
Sullivan M. et al., 2010, MNRAS, 406, 782
Torrado J., Lewis A., 2021, J. Cosmol. Astropart. Phys., 05, 057
Verde L., Protopapas P., Jimenez R., 2013, Phys. Dark Universe, 2, 166
Vincenzi M. et al., 2024, ApJ, 975, 86
Wang J., Huang Z., Huang L., 2023, Sci. China Phys. Mech. Astron., 66, 129511
Wiseman P. et al., 2021, MNRAS, 506, 3330
Wiseman P., Sullivan M., Smith M., Popovic B., 2023, MNRAS, 520, 6214
Zhang K. D., Murakami Y. S., Stahl B. E., Patra K. C., Filippenko A. V., 2021, MNRAS, 503, L33

This paper has been typeset from a TEX/LATEX file prepared by the author.